Development of Polysulfone-Nanohybrid Membranes using ZnO-GO composite for enhanced antifouling and antibacterial control

Ying Tao Chung [a], Ebrahim Mahmoudi [a], Abdul Wahab Mohammad [a,b*], Abdelbaki Benamor [c], Daniel Johnson [d] and Nidal Hilal [d]

[a] *Department of Chemical and Process Engineering, Faculty of Engineering and Built Environment, Universiti Kebangsaan Malaysia, 43600 Bangi, Selangor Darul Ehsan, Malaysia.*
[b] *Centre for Sustainable Process Technology (CESPRO), Faculty of Engineering and Built Environment, Universiti Kebangsaan Malaysia, 43600 Bangi, Selangor Darul Ehsan, Malaysia.*
[c] *Gas Processing Centre, Qatar University, P.O. Box 2713, Doha, Qatar.*
[d] *Centre for Water Advanced Technologies and Environmental Research (CWATER), College of Engineering, Swansea University, Swansea SA2 8PP, United Kingdom.*

*****Corresponding author. Tel: +6 03 89118000; Fax: +6 03 89252546; E-mail: drawm@ukm.edu.my

HIGHLIGHTS

- Various percentages of minimal-size ZnO and ZnO-GO for PSF membrane enhancement.
- 5 times reduction of ZnO usage with the introduction of GO nanosheets as support.
- ZnO-GO composite is more hydrophilic compared to other GO-nanohybrid.
- ZnO-GO membrane exhibits excellent antifouling and antibacterial properties.

ABSTRACT

Zinc oxide nanoparticles were well-known for the enhanced antifouling and antibacterial properties which could be beneficial for membrane processes in desalination. The functionalization of ZnO onto graphene oxide nanoplates was targeted for better distribution. Both ZnO and ZnO-GO NPs were synthesized using sol-gel method. The nanoparticles characteristics were checked with XRD, TEM, and FESEM. The nanohybrid membranes were fabricated via wet phase inversion technique and embedded with various percentage of ZnO (1, 2, 3 wt %) and ZnO-GO (0.1, 0.3, 0.6 wt %) nanoparticles. All the membranes with nanoparticles incorporation exhibited improved membrane properties in comparison with the pristine PSF membrane. The best membrane performance was shown in membrane with 2 wt% of ZnO and 0.6 wt% of ZnO-GO. These two membranes presented significantly improved performance such as enhanced hydrophilicity, high permeability and porosity, improved humic acid rejection rate as well as good antifouling and antibacterial control. To an extent, the excellent antimicrobial ability of these nanohybrid membranes appeared as appropriate candidate to contribute or overcome bio-fouling issues in applications such as brackish water or seawater desalination. Hence, ZnO and ZnO-GO NPs were superb nanomaterials in the fabrication of PSF-nanohybrid membranes. The use of GO nanoplates allowed reduction of ZnO composition by up to 5 times while showing similar performances.

Keywords: Zinc oxide; Zinc oxide-Graphene oxide nanohybrid; Polysulfone membrane; Antifouling; Antibacterial

1. Introduction

Membrane fouling has been a major obstacle in water and wastewater treatment industry since decades ago. This weakness would impose problems in the separation process efficiency and lead to frequent maintenance of membrane operations [1]. A variety of researches has been performed to overcome the fouling issues. Several membrane modification methods have been practised widely to improve the membrane performance, i.e. development of composite membranes via interfacial polymerization [2], UV-initiated grafting [3], plasma treatment [4], electron beam irradiation [5] , layer-by-layer deposition [6] and incorporation of nanoparticles or antifouling agents [7]. In recent years, membrane separation advances have been achieved by introducing the application of nanomaterials in membranes. The combination of membrane and nanotechnology could lead to new breakthrough in the membrane development industry due to its versatile and attractive advantages.

To date, the establishment of nanoparticles-embedded membranes is attaining tremendous interest due to its ability to enhance properties of membranes. Nanoparticles (NPs) which span the range between 1 nm to 100 nm are the most fundamental component in the formation of a nanostructure. According to Horikoshi et al., metallic NPs would normally yield different characteristics from bulk metals, in which the nano-size particulates would exhibit greater physical and chemical properties due to the enhanced surface area [8]. Numerous types of metal or metal oxide NPs have been reportedly used in membrane applications, such as silver (Ag), iron (Fe_2O_3, Fe_3O_4), silica (SiO_2), aluminium (Al_2O_3), titanium (TiO_2), magnesium oxide (MgO), and zirconium dioxide (ZrO_2) [7]. Some of these metal oxide NPs are quite expensive and thus efforts have been focused to opt for a lower cost metal oxide. One of the popular low-cost metal oxide is zinc oxide (ZnO), which has been used as a new alternative for titanium oxide replacement [9].

ZnO NPs are gaining rising attention in various industrial applications such as biomedical, optics, electronics, and recently in the development of membrane technology, owing to their superb antimicrobial, anti-corrosive, thermal and mechanical stability properties [10]. Several researches have been reported on the incorporation of various concentrations of ZnO NPs into different polymer matrix such as Polysulfone (PSF), Polyether sulfone (PES) and Polyvinylidene fluoride (PVDF). These studies reported on the formation of ultrafiltration (UF) and tight UF membranes with improved membrane performances such as

higher permeability, rejection capability, porosity, hydrophilicity and enhanced antifouling properties [11],[12],[13]. In addition, the ZnO-incorporated membranes also exhibited essential heavy metal ions (Cu^{2+}) adsorption [14], reduced oleic acid fouling [15], improved dye rejection ability [9], collagen separation [16] and excellent photo-catalysis self-cleaning [17]. These interesting findings indicated that ZnO NPs has the potential to be an excellent NP candidate for better membrane quality.

Although ZnO NPs yielded outstanding characteristics in membrane fabrication, there are drawbacks and limitations. This is a common issue for NPs incorporation, due to the nano-size particulates aggregation and formation of non-homogeneous distribution during the membrane formation. Therefore, graphene oxide (GO) nanosheets have been introduced as a versatile platform for better nanomaterials dispersion and appeared as an innovative material in membrane preparation [18][19]. This has been contributed by the synergistic effects between the hydrophilic-layered GO and nanoparticles. The carboxylic and hydroxyl functional groups of GO are essential in forming hybrid nanostructures with various kinds of NPs such as Ag, SiO_2, TiO_2 and so forth [20]. For instance, the synthesis of silver-graphene oxide (Ag/GO) nanocomposites has been reported as vital antibacterial agent for water disinfection [18]. According to Sun et al., the Ag/GO nanocomposite has been further developed in membrane fabrication for water purification [21]. The novel mixed matrix UF membrane impregnated with Ag/GO also exhibits excellent antifouling and anti-biofouling properties [22]. In addition, the unique nanohybrid SiO_2/GO PSF membranes revealed significant improvement in terms of flux, protein rejection and antifouling tendency [23]. Furthermore, the nanocomposite of TiO_2/GO PES membrane also illustrated perfect nanofiltration membrane performance in various aspects such as water permeability, hydrophilicity, fouling resistance and dye retention [24]. Similar improved desalination performance by TiO_2/GO nanocomposite reverse osmosis membranes were developed too [25]. Besides, the formation of ZnO-GO composite has been shown to have better photocatalytic activity [26]. However, the study of ZnO-GO composite in membrane fabrication is still limited.

Hence, the ultimate goal of this study is to develop PSF membranes with ZnO NPs and ZnO-GO nanohybrid in order to obtain improved membrane performance with enhanced permeability rate, rejection capability as well as fouling propensity. The ZnO NPs agglomeration problem is aimed to be overcome by decorating ZnO NPs onto the surface of GO nanosheets. The amount of ZnO could also be reduced by dispersing it on GO nanosheets.

The PSF-GO membranes is not included in this study as the literature shows that the GO-nanohybrid membranes are always exhibiting better performance in comparison with GO membranes [23][27][28][29]. Therefore, the focus of the study will be the investigations on the comparison between the incorporation of minimal-size ZnO NPs and functionalized ZnO with GO nanosheets towards the membrane performance. The membrane overall performance will be further characterized by several approaches, i.e. water permeability test, humic acid rejection, hydrophilicity study, porosity analysis, morphology study with Field Emission Scanning Electron Microscopy (FESEM) and Atomic Force Microscopy (AFM). Finally, the antifouling and antibacterial analysis will be performed to determine the Polysulfone-nanohybrid membranes workability and efficiency in fouling resistance and bio-fouling control for further applications such as separation, purification, desalination as well as water and wastewater treatment.

2. Experimental

2.1. Materials

Polysulfone (PSF) granules were obtained from Goodfellow Cambridge Ltd., England. The solvent 1-methyl-2-pyrrolidinone (NMP, 99.5% purity) was of analytical grade and purchased from Merck Co., Germany. Humic acid was supplied by Sigma Aldrich Co., USA. All chemicals were used without any further purification.

2.2. Synthesis of ZnO and ZnO-GO Nanoparticles

ZnO NPs were prepared through sol-gel method with average size of 13 nm as reported in detail in our previous study [30]. Graphene oxide (GO) was synthesized from natural graphite powder based on Hummers method, as described in previous study [29]. The ZnO-GO nanohybrid was produced via sol-gel method by decorating 20 wt% of ZnO onto the GO nanosheets support. Finally, the mixture was centrifuged and dried with oven overnight before calcination.

2.3. Nanoparticles characterization

The crystallite size of the ZnO nanoparticles and crystal phase composition could be analysed by performing X-ray diffraction (XRD; Bruker D8 Advance AXS X-ray diffractometer) with CuKα radiation(1.5406 Å) in the 2h scan range of 20–80^{o}. The average crystallite size of the ZnO was obtained from the XRD patterns with the Debye–Scherer equation Eq. (1).

$$D = K\lambda / \beta\cos\theta \quad (1)$$

where K is the Scherer constant (K = 0.89), λ is the X-ray wavelength, β is the peak width at half maximum, and θ is the Bragg diffraction angle. Besides, the ZnO nanoparticles crystallite size was observed using a transmission electron microscope (TEM; Philips CM200, model JEOLJEM 2100). The nanoparticles' morphology structure were further determined using high resolution field emission scanning electron microscopy (SEM; SUPRA 55VP) with energy-dispersive X-ray spectroscopy (EDX) (Oxford EDX INCA Penta FETX3).

2.4. Membrane Fabrication

Phase inversion technique was applied in the membrane fabrication. Various percentages of ZnO and ZnO-GO NPs were incorporated during the preparation of PSF casting solution. The casting solution was prepared by dissolving 20 wt% of PSF pellets into NMP with average

temperature of 60±5 °C under continuous stirring for 5 hr. The NPs were sonicated for 30 mins to ensure better dispersion before mixing in the homogeneous PSF casting solution. The membranes were cast by using Filmographe Doctor Blade 360099003 (Braive Instrument, Germany) with thickness of 0.2 mm. The coagulation process of membrane occurred in a 25°C water bath. The fabricated membranes were then kept overnight with ultrapure water for storage.

2.5. Membrane performance testing and characterization

2.5.1. Hydrophilicity study

The angle between water and membrane surface was measured with contact angle meter (Model Kruss GmbH, Germany with Drop Shape Analysis software). The membrane surface hydrophilicity was measured for 3 times and compared according to the contact angle values for each membrane.

2.5.2. Permeability test

Membrane permeability was determined by measuring the pure water fluxes using a stirred cell (Sterlitech HP4750). The pure water flux was calculated by using the following equation:

$$J = V / s\,t \tag{2}$$

where J is the water flux (L m^{-2} hr^{-1}); V is the permeate volume (L); s is the effective membrane area (m^2); t is the operation time (hr). Data of water fluxes against pressures was plotted and the permeability was determined according to the gradient of the linear line. The permeate was also analysed for the presence of Zn using Inductively Coupled Plasma Mass Spectrometry (ICP-MS) analysis (PerkinElmer, Model ELAN 9000). This is to check whether nanoparticle leaching took place. The ICP-MS analysis confirmed that there was no nanoparticle leaching after permeation of pure water.

2.5.3. Porosity analysis

Membrane porosity (ε) was analysed by performing gravimetric method, as shown in the following equation:

$$\varepsilon = \frac{\omega_1 - \omega_2}{A \times n \times d_w} \tag{3}$$

where ω_1 is the wet membrane weight and ω_2 is the dried membrane weight, A(m^2) is the area of the membrane, n is the thickness and d_w is the water density (998 kg/m^3). Besides,

membrane pore size could be estimated by using the porosity data and Guerout–Elford–Ferry equation in Eq. (4).

$$r_m = \sqrt{\frac{(2.9 - 1.75\varepsilon)8\eta lQ}{\varepsilon \times A \times \Delta P}} \quad (4)$$

where η is the water viscosity (8.9×10^{-4} Pa s), Q is the volume of permeated pure water per unit time (m^3/s), and ΔP is the applied pressure (MPa).

2.5.4. Morphological study

The surfaces and cross-sectional structures of the pure and modified membranes were observed by using Field Emission Scanning Electron Microscope (FESEM, Gemini SUPRA 55VP-ZEISS). Mapping analysis was performed by using Aztec ver.3.0 software. Besides, membrane surface roughness was determined by applying Multimode AFM with Nanoscope IIIa controller (Veeco, USA), under ambient conditions using tapping mode with TESP cantilevers (Bruker AXS). The scanned area was 10 x 10 μm.

2.5.5. Rejection study & Antifouling testing

Rejection study of membranes was performed by using 10ppm of humic acid solution. The rejection was determined by using the following equation:

$$R = (1 - C_p/C_f) \times 100\% \quad (5)$$

where C_p is the permeate solution concentration and C_f is the feed solution concentration.

The flux decline profile was analysed by plotting normalized flux against time. Besides, flux recovery ratio (FRR) was determined after the fouling test where the fouled membrane will be rinsed with ultrapure water for about 30 minutes. The flux recovery could be calculated by using the equation (6):

$$FRR = (J_2 / J_1) \times 100\% \quad (6)$$

where J_1 is the pure water flux before fouling test and J_2 is the pure water flux after fouling.

Besides, the relative flux reduction ratio (RFR) was calculated by the following equation:

$$RFR = (1 - J_P / J_1) \times 100\% \quad (7)$$

where J_P is the foulant flux and J_1 is the pure water flux.

2.5.6. Antibacterial testing

Antibacterial testing of the membranes was performed by using Escherichia coli (E.coli). Initially, E.coli was cultured in nutrient broth to obtain a stock with 109 CFU/ml. Next, the

stock solution was further diluted into 20 CFU/ml from the stock nutrient broth. Membranes were sent for autoclave before testing and were dipped into the diluted E.coli solution for about 10 min. The membranes were then placed on nutrient agar plates and incubated overnight. Finally, the colony forming units (CFUs) of E.coli on the membrane surface were observed using FESEM [29].

3. Results and discussion

3.1. Nanoparticles characterizations

The ZnO and ZnO-GO NPs were successfully synthesized via sol-gel technique. The produced NPs were verified and confirmed with several characterization methods to ensure the originality of the NPs. Hence, XRD, TEM, FESEM with EDX were carried out to assess the purity of NPs.

3.1.1. XRD

Firstly, the purity and crystallite size of ZnO and ZnO-GO NPs were confirmed by XRD analysis. Fig. 1 illustrated all the diffraction peaks existing in ZnO and ZnO-GO NPs. It was confirmed that the synthesized ZnO NPs were in hexagonal phase with wurtzite structure, complimentary with the data in JCPDS card No.36-1415 with Miller indices (1 0 0), (0 0 2), (1 0 1), (10 2), (1 1 0), (1 0 3), (1 1 2), (2 0 1) and lattice parameters, a = b = 0.3249 nm and c = 0.5206 nm [31]. The crystallite size was calculated based on the Debye–Scherer equation, in which the size existed in range of 10-20 nm. On the other hand, the XRD spectra of ZnO-GO NPs exhibited the presence of reduced GO peak in the range of 20-30° as reported elsewhere [32],[33]. The spectrum proved the integration between GO and ZnO NPs.

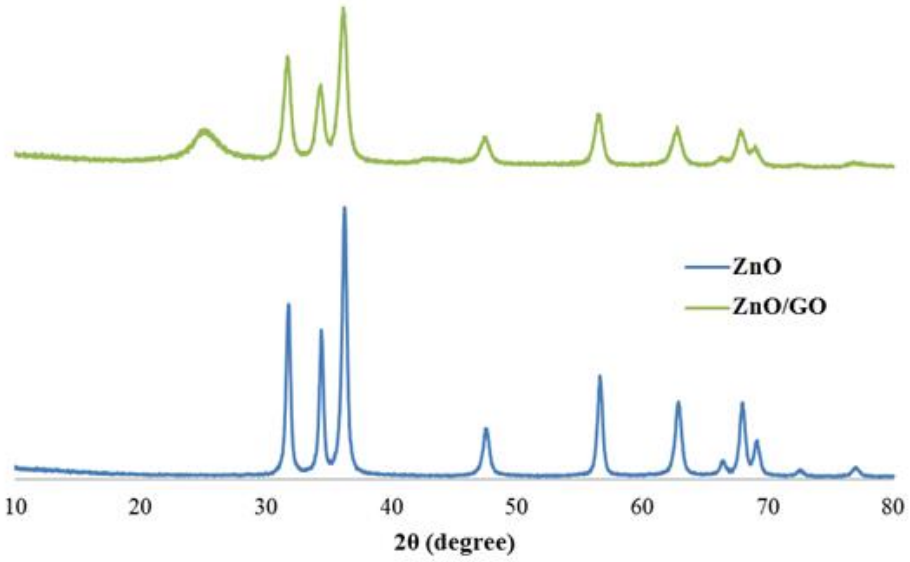

Fig. 1. XRD peaks for ZnO and ZnO/GO NPs.

3.1.2. TEM

As a supporting analysis for the NPs size and shape confirmation, TEM analysis was carried out for the synthesized ZnO and ZnO-GO NPs. Fig. 2 (a) and (b) showed that the average particles size of both synthesized ZnO and ZnO-GO NPs was within the range of 10 - 15nm [30]. It was in good agreement with the XRD size prediction. Besides, it was observed that there was uniform distribution of spherical-shaped ZnO NPs on the GO nanosheets shown in Fig. 2(d) in comparison with the ZnO NPs shown in Fig. 2(c) which showed slight agglomerations. It was a good phenomenon as the evenly-distributed ZnO NPs decorated onto GO nanoplates would impose great enhancement for incorporation into the membrane structures.

3.1.3. FESEM & EDX

In addition, Fig. 2 (c) to (f) demonstrated the FESEM with EDX analysis as final confirmation for the morphology and elemental study of ZnO and ZnO-GO NPs. Similar to the TEM figures, the morphological study with FESEM was compatible and exhibited the consistency in the distribution ZnO and ZnO-GO NPs. EDX spectrum was another important tool to examine the elemental composition of the synthesized NPs. The elements of interest for ZnO were zinc and oxygen while ZnO-GO composite were zinc, oxygen and carbon. Apparently, both EDX spectra reflected the presence of high abundance of listed elements in both synthesized NPs which further confirmed the purity of the NPs. The composition of

ZnO NPs consisted of 74 wt% of Zn and 15 wt% of O while ZnO-GO were formed by 60 wt% of C, 24 wt% of Zn and 16 wt% of O. Hence, it could be concluded that the synthesized ZnO and ZnO-GO NPs were high in purity with consistent particles size.

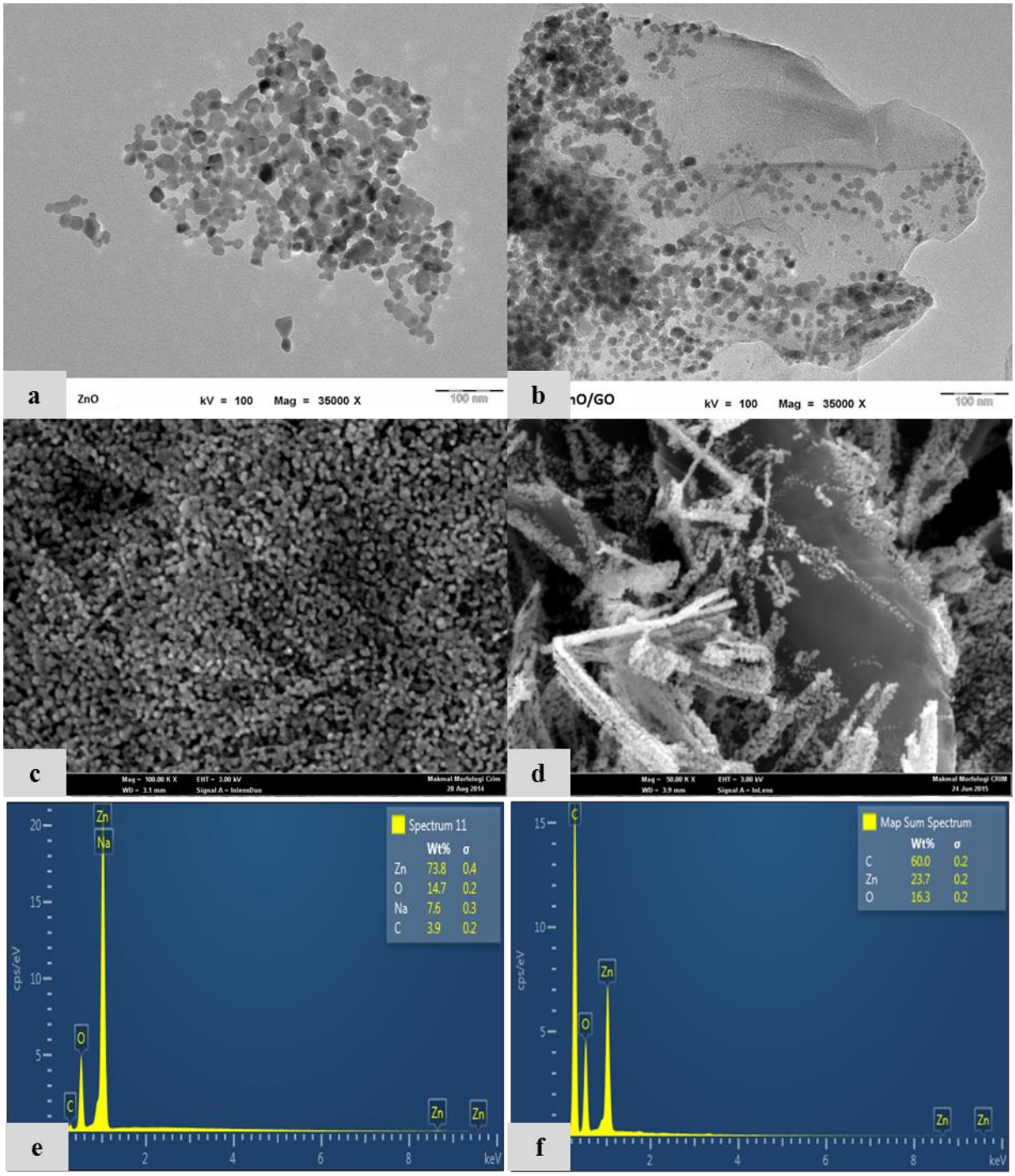

Fig. 2. TEM images: (a) ZnO, (b) ZnO-GO; FESEM images: (c) ZnO, (d) ZnO-GO and EDX spectra: (e) ZnO, (f) ZnO-GO.

3.2. Membrane performance testing and characterization

After confirming the characteristics of the ZnO and ZnO-GO NPs, these NPs were applied in membrane fabrication via phase inversion technique. To provide further insight of PSF membranes performance with these nanohybrids, the comparison of various concentrations of ZnO [1, 2, 3 wt%] and ZnO-GO [0.1, 0.3, 0.6 wt%] was performed. The nanohybrid membranes were then characterized by several methods such as surface hydrophilicity, permeability testing, porosity, rejection, morphological study and so forth. Table 1 listed the polymer, solvent and nanoparticles ratio for the membrane fabrication.

Table 1.

Ratio of polymer, solvent and nanoparticles percentage.

Membrane	NPs percentage (wt %)	Mass ratio of PSF:NMP:NPs
P0	-	1:5:0
Z1	ZnO 1%	1:5:0.01
Z2	ZnO 2%	1:5:0.02
Z3	ZnO 3%	1:5:0.03
ZG1	ZnO-GO 0.1%	1:5:0.001
ZG2	ZnO-GO 0.3%	1:5:0.003
ZG3	ZnO-GO 0.6%	1:5:0.006

3.2.1. Permeability & Hydrophilicity

First of all, the performance of the nanohybrid membranes was characterized through water permeability and contact angle testing. Water permeability testing was evaluated based on flux while contact angle was an important indicator for membrane hydrophobicity or hydrophilicity. The correlation between both responses was visualised in Fig. 3. In general, the permeability of membrane correlated disproportionately with membrane hydrophilicity. This was an interesting finding which marked the significance of ZnO and ZnO-GO NPs in improving membrane performance. There was also an obvious trend which showed the decrement in contact angle value with increased amount of either ZnO or ZnO-GO NPs in comparison with pure PSF membrane (P0). The lower the contact angle value, the better the hydrophilicity of membrane [29]. As shown in Fig. 3, the contact angle value declined from 65.9 ^{o} to 39.6 ^{o} with the addition of various amount of ZnO and ZnO-GO NPs. There was not

much difference of average contact angle values between several concentrations of both ZnO and ZnO-GO NPs membranes, considering the standard deviation. It was mainly due to the contact angle test was only performed using water droplet on the surface of membranes, regardless the exact loading of ZnO and ZnO-GO nanostructures. However, the result was satisfactory due to the enhanced hydrophilic nature of the membranes compared with the bare PSF membrane. The improved hydrophilicity could be explained by the reduced interface energy of the mixed matrix membranes affected by the polar characteristics of ZnO NPs and large abundance of polar functional groups on the surface of GO nanosheets [34][35]. It was well known that hydrophilicity correlated directly with membrane permeability. All of the nanohybrid membranes yielded higher permeability than the pure PSF membrane due to the synergistic effects between polymer and nanofillers which was similar to other nanohybrid membrane studies [23]. The best enhancement of both types of nanohybrid membranes was demonstrated in membranes with loadings of 2 wt% ZnO (Z2) and 0.6 wt% of ZnO-GO (ZG3). Interestingly, the permeability of membranes increased from 0.89 to 2.83 and 5.11 $L.m^{-2}.h^{-1}.bar^{-1}$ for membrane P0, Z2 and ZG3 respectively. It was an improvement for a multiple of five which significantly highlighted the vital role of hydrophilic nanostructures in contributing to the membrane permeability. Besides, the solvent and non-solvent exchange rate during the phase inversion process was an important factor leading to better membrane permeability. The hydrophilic nature of ZnO and ZnO-GO NPs would greatly enhance the viscosity casting solution and accelerate the solvent/non-solvent exchange rate [36]. Hence, it was in good agreement with the theory of enhanced diffusion rate with less viscous blending solution would produce highly permeable membranes [13].

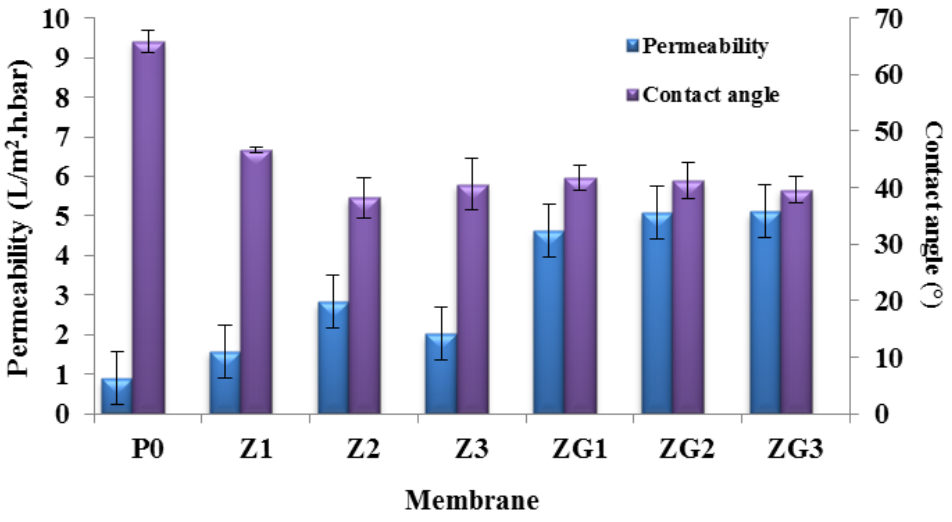

Fig. 3. Permeability and hydrophilicity of the membranes.

3.2.2. Porosity and pore size

Generally, membrane porosity was dependent on the mass transfer of the polymer solution during the phase inversion process [17]. Referring to the discussion on membrane hydrophilicity, the hydrophilic nature owned by the ZnO and ZnO-GO nanohybrids did contribute significantly to the membrane porosity. The hydrophilic functional groups from the nanohybrids would accelerate the membrane formation process by speeding up the exchange rate between solvent and non-solvent. Therefore, the pores formation process would be enhanced. As shown in Table 2, the porosity of membranes increased from 75% for bare PSF (P0) membrane to 86% for PSF-ZnO (Z2) membrane and the highest porosity of 90% for PSF-ZnO-GO (ZG3) membrane. The porosity result was excellent in comparison with some of the literature [37][27]. All the modified membranes porosity was improved but there was only a little difference between various loadings of ZnO and ZnO-GO nanomaterials. The slight decrement of porosity for Z3 membrane might be caused by the pores blockage due to the high concentration of ZnO NPs [27]. The enhancement of porosity for nanohybrid membranes were attributed to the less viscous blending solution with hydrophilic ZnO and ZnO-GO which directly led to faster occurrence of phase inversion process [38]. In addition, the membranes average pore size was estimated to enlarge from 2 nm to 4 nm. Although the variance of pores sizes was not significant, it could be concluded that all the membranes were approaching nanoscale which was a promising step to the formation of nanofiltration membrane in accordance to the permeability, too [15].

Table 2.

Porosity and pore size of membranes.

Membrane	Porosity, ε %	Pore size, nm
P0	75.2	2.04
Z1	85.3	2.12
Z2	86.7	3.19
Z3	84.2	2.77
ZG1	80.9	4.03
ZG2	86.2	4.39
ZG3	90.0	4.09

3.2.3. Morphological study

Morphological analysis was equally important to provide a better insight for the development of membranes. Generally, the surface, cross-sectional, EDX and mapping analysis were performed by applying FESEM to examine the formation of membrane structures. The morphology of membranes were affected by several factors including the interaction, viscosity and diffusion rate of the casting solution [37]. The rate of solidification and coagulation of PSF polymer would decide the membrane matrix formation [13]. Fig. 4 displayed the entire surface, cross sectional and EDX images for the pristine PSF (P0), PSF-ZnO (Z2), and PSF-ZnO-GO (ZG3) membranes. The membrane surface shown in Fig. 4(a)-(c) indicated the P0 membrane had rougher surface, possibly due to the formation of biofilm. The membrane matrices were basically formed with a dense top layer and a porous support layer [27]. The P0 membranes possessed more sponge-like structures at the bottom layer and a thickened top layer due to its delayed demixing rate which slower the phase inversion process. On the other hand, it was notable that the Z2 and ZG3 membranes cross sections exhibited finger-like structures which were likely due to the improved diffusion rate of the casting solution as per reported elsewhere [37]. The ZG3 membrane which was incorporated with ZnO NPs decorated on the GO nanosheets presented more finger-like channels with abundance of macrovoids at the membrane sub layer [24]. As a result, the number and size of pores were enhanced which was in good agreement with the porosity findings discussed above [20]. Hence, the Z2 and ZG3 membranes were selected for better enhancement of water permeability with increased porosity and pore size. In addition, the EDX analysis was rather important to verify the elements presented in the membrane matrix. As shown in Fig. 4 (g)-(i), all the membranes were examined for the presence of the Carbon, Oxygen, Sulphur and Zinc components. The Zinc element was not detected in P0 membrane but in Z2 and ZG3 membranes, whereas the other elements were detected in all the 3 membranes with various percentages, in which the Carbon element was the highest amount in ZG3 membrane due to the presence of GO nanosheets. Finally, the mapping analysis was carried out for both Z2 and ZG3 membrane to check the distribution of each of the elements in membrane structure. Fig. 5 illustrated the distribution of Carbon, Oxygen, Sulphur and Zinc composition in membranes. Interestingly, the Zinc elements exhibited well and homogeneous dispersion without any agglomerations. This was an encouraging phenomenon as the conglomerations problem of nanoparticles could be greatly enhanced with the introduction of GO nanosheets as a better nanoparticles' dispersing platform [23].

In addition, the surface morphology of the fabricated membranes was also performed with AFM analysis. Fig. 6 (a)-(c) illustrated the three-dimensional images of the three synthesized membranes, i.e. P0, Z2 and ZG3 membranes. The table in Fig. 6 (d) also presented the surface roughness values of the membranes. It was known that the surface with more peaks or valleys represented rougher membrane surface. As shown in Fig 6, the AFM image coincided well with mean RMS values which marked the higher surface roughness of P0 membrane in comparison with Z2 and ZG3 membranes. The addition of ZnO and ZnO-GO NPs altered the membrane structure and turned the larger peaks or valleys of the membranes into smaller valleys. Eventually, the embedment of GO nanoplates would assist in creating smoother membrane surface due to the low electrostatic interaction and high compatibility with PSF membrane matrix [27]. The findings were similar with some previous studies [37][39]. Generally, higher surface roughness would normally result in a higher fouling tendency and hydrophobicity. This phenomenon could be further explained by Wenzel's model, in which the degree of roughness correlated proportionally to the surface hydrophilicity or hydrophobicity [40]. Hence, the incorporation of ZnO and functionalized ZnO nanomaterials would definitely enhance the membrane properties by providing smoother membrane structure.

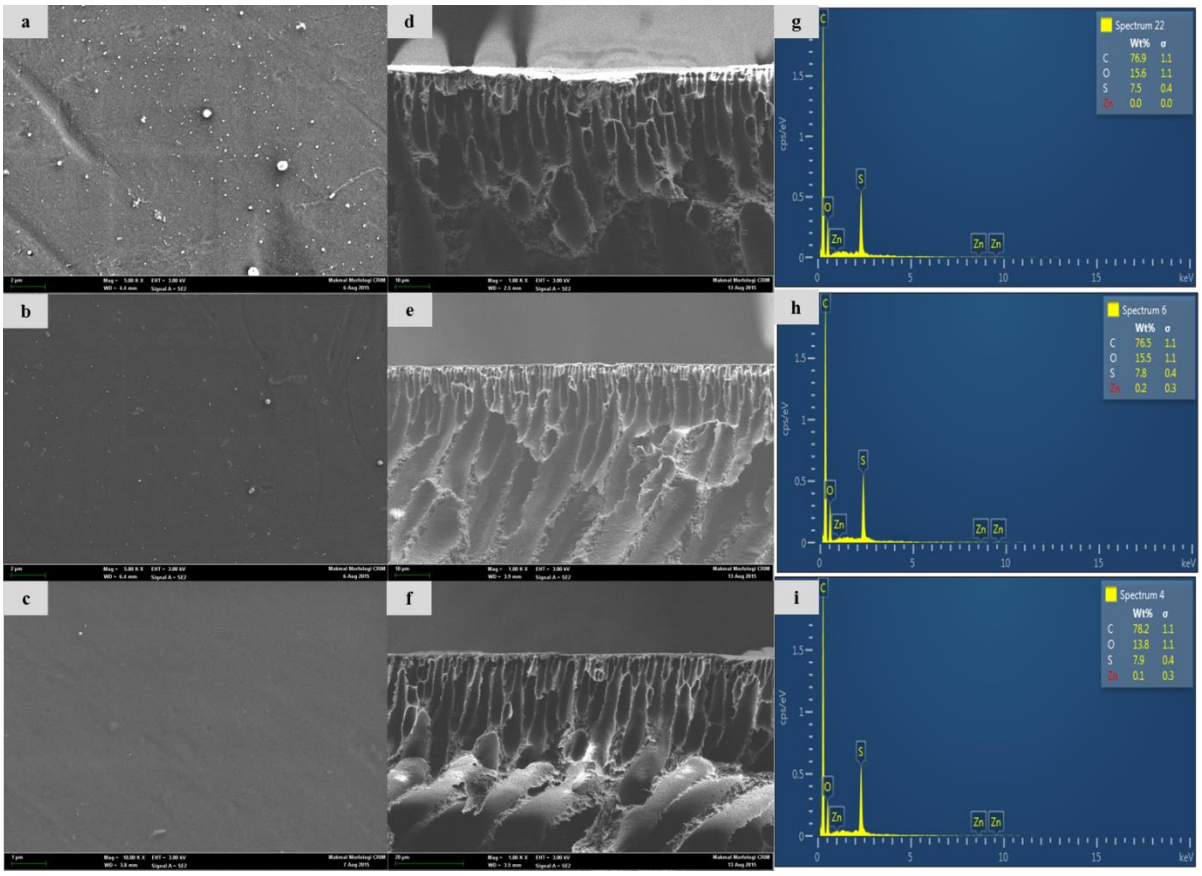

Fig. 4. FESEM images of membranes: [i] Surface: (a) P0 (b) Z2 (c) ZG3; [ii] Cross sectional: (d) P0 (e) Z2 (f) ZG3; [iii] EDX spectra: (g) P0 (h) Z2 (i) ZG3.

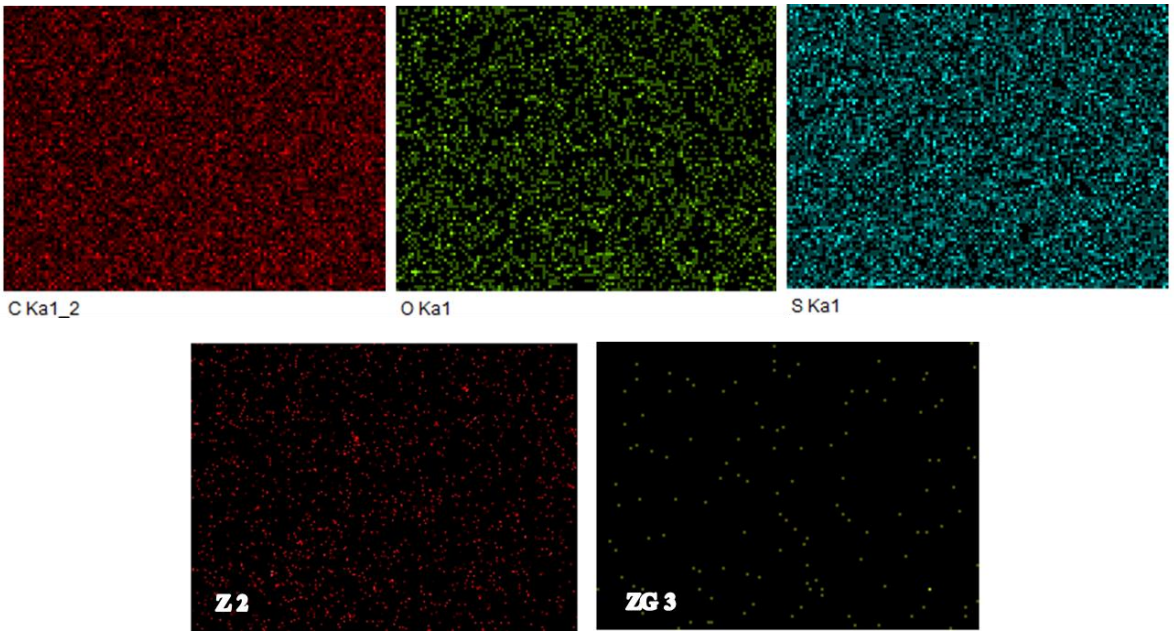

Fig. 5. FESEM mapping images for Z2 and ZG3 membrane.

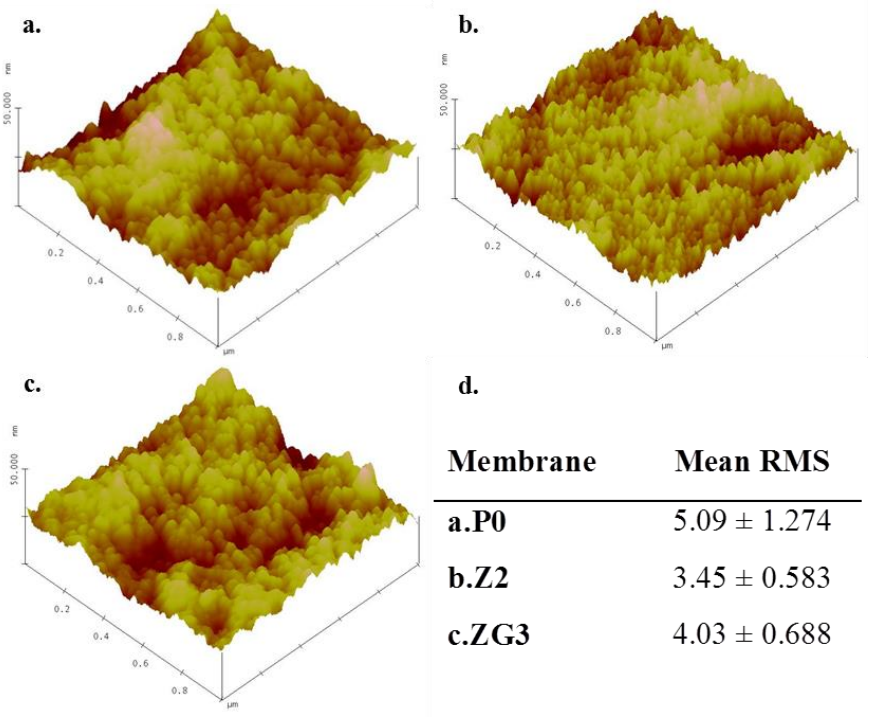

Membrane	Mean RMS
a.P0	5.09 ± 1.274
b.Z2	3.45 ± 0.583
c.ZG3	4.03 ± 0.688

Fig. 6. AFM images and surface roughness analysis for membranes: a) P0 b) Z2 c) ZG3; d) Mean RMS value.

3.3. Membrane Application

Knowing the excellent characteristics of the fabricated membranes, the antifouling and antibacterial evaluations were then performed to assess the workability and efficiency of the membranes. The antifouling testing would be assessed by applying humic acid solution as organic foulants while antimicrobial analysis were examined by using *Escherichia coli* (E.coli). These analyses were important in membrane development due to the critical issues of fouling and bio-fouling.

3.3.1. Antifouling properties

The rejection tendency of all the fabricated membranes [P0-ZG3] was checked by applying humic acid solution as organic foulants. Based on Fig. 7, the rejection percentage of humic acid increased from 52% for P0 membrane to 99% for ZG3 membrane. The Z2 and Z3 membranes indicated equally great rejection propensity with ZG3 membrane. However, ZG3 membrane exhibited outstanding performance with high permeability and simultaneously excellent rejection capability. This was an encouraging finding to prove that the enhanced antifouling properties of membranes incorporated with both ZnO and ZnO-GO NPs. This phenomenon was possibly attributed to the hydrophilic nature of the ZnO and ZnO-GO which would reduce the adsorption of organic pollutants within the membrane structure [9]. The improved hydrophilicity originated from the high polarity ZnO NPs and the abundance of hydroxyl, carbonyl and epoxy functional groups on the GO nanosheets [41] which could reduce the adsorption of humic acid molecules onto membranes surface [42]. The establishment of highly hydrophilic membrane structure with ZnO and ZnO-GO composites was aimed to increase the affinity of these NPs to water rather than the organic matter, resulting in lower hydraulic resistance [38]. Hence, there would be higher retention of foulants by utilizing the membranes embedded with highly hydrophilic ZnO-GO NPs.

After conducting the rejection analysis, flux decline against time profile was plotted to evaluate the antifouling performance of membranes. As shown in Fig. 8, the normalized flux decline analysis was performed on 3 selected membranes, i.e. pure PSF membrane (P0), PSF-ZnO (Z2) and PSF-ZnO-GO (ZG3). The normalized plot behaviour, as referred to Fig 3, exhibited that membranes with greater hydrophilicty yield higher J/J_o value. The flux decline analysis indicated that Z2 and ZG3 membranes possessed better antifouling ability in comparison with the P0 membrane. To an extent, this could be explained by the correlation between hydrophilicity of membrane and degree of fouling. The higher the hydrophilicity of

membranes, the greater their resistances towards fouling matter In brief, it could be summarized that the antifouling behaviour was very much dependent on the hydrophilic nature of membranes which were altered by the oxygenated groups from the ZnO-GO nanohybrids [39]. [43]. Besides, the normalized flux was more than 1 for Z2 and ZG3 membrane, possibly due to the existence of ZnO nanohybrid which might affect the membrane properties and resulted in higher normalized flux value. As shown in Fig.9, the flux profile demonstrated the complete cycle of antifouling test, in which ZG3 membrane had better recovery as the W2 region was still fluctuating in a consistent value in comparison to Z2 and P0 which showed a slight decrease trend after the HA fouling test. This phenomenon was possibly due to the deposition of HA onto the membrane surface which led to the decrement of flux. With the introduction of ZnO decorated on GO nanosheets (ZG3 membranes), the synergistic effect of both nanomaterials enhanced the surface hydrophilicity and therefore it contributed to the antifouling ability towards the organic foulant. The common way to investigate fouling resistance was by determining the flux recovery ratio (FRR). Fig. 10 presented the flux recovery ratio (FRR %) and relative flux reduction ratio (RFR %) of the 3 types of membranes. The higher RFR ratio represented the membrane was prone to fouling which led to significant flux decline during the fouling test. From Fig. 10, P0 membrane showed higher RFR value in comparison with Z2 and ZG3 nanohybrid membranes. This was explained by the additional of nanohybrid materials would prevent the membranes from fouling and reduced the flux reduction. On the other hand, the FRR trend signified that ZG3 membrane had the best flux recovery ratio. This was likely due to the surface roughness of the membranes. The lower roughness of membranes would contribute to the better of FRR [39]. This was proven with the AFM analysis with surface roughness parameters.

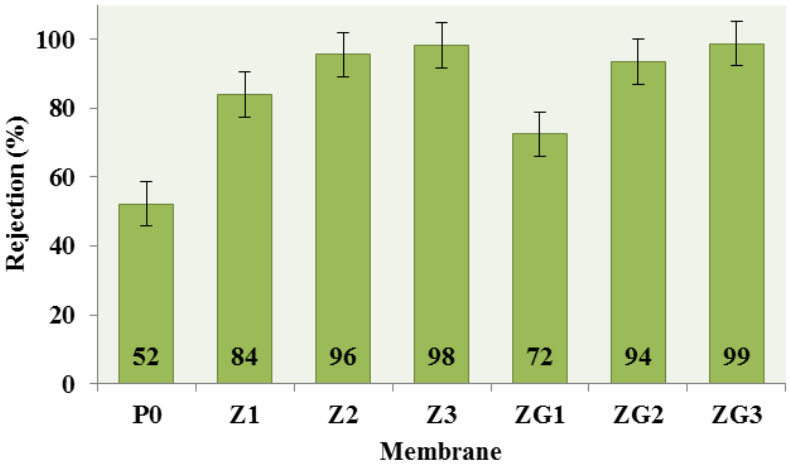

Fig. 7. Humic acid rejection percentage.

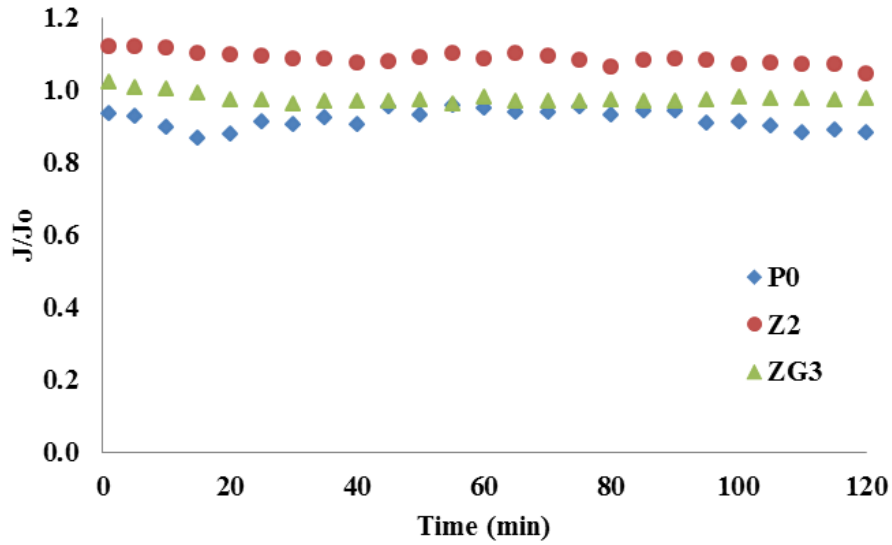

Fig. 8. Normalized flux decline analysis of membranes.

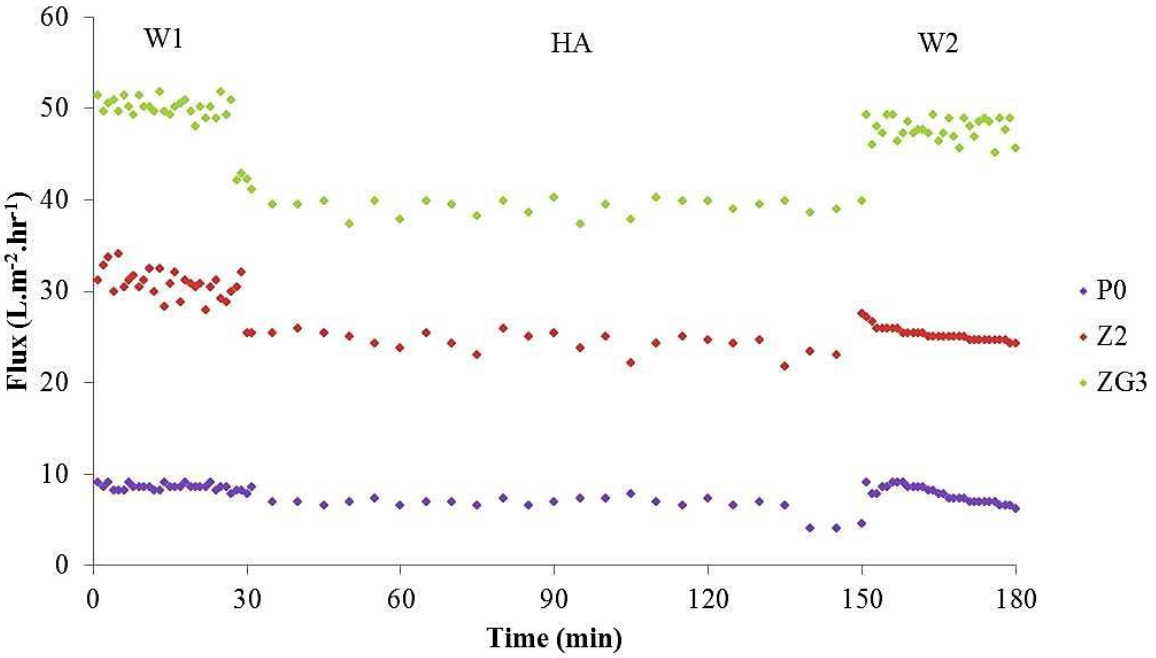

Fig. 9. Flux profile with water and humic acid: W1: pure water flux for 30mins; HA: Humic acid for 2 hr; W2: pure water recovery for 30 mins.

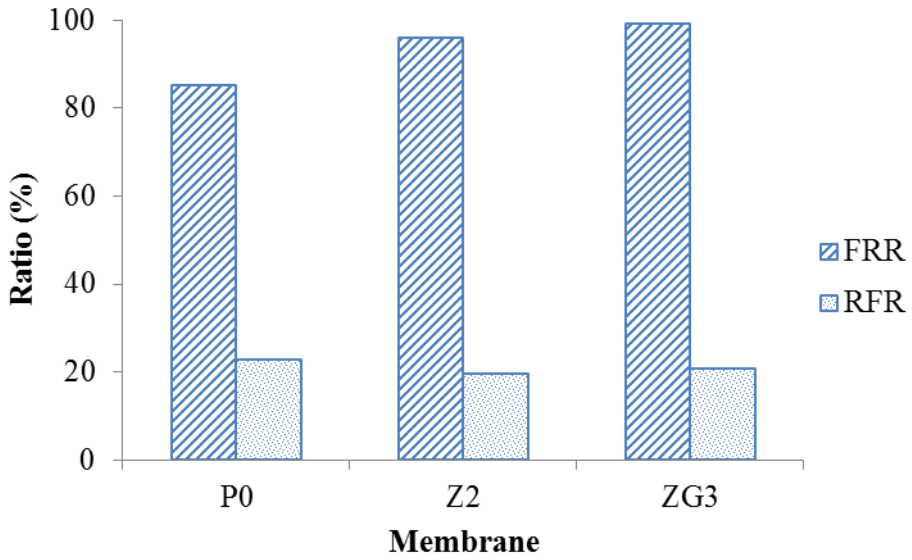

Fig. 9. Flux recovery ratio (FRR) and Relative flux reduction ratio (RFR)

3.3.2. Antibacterial properties

ZnO NPs had gained significant interest in bio-fouling studies since it was a bio-safe material which could act as outstanding antimicrobial agents in various applications [44]. It was also well known that ZnO NPs possessed excellent antimicrobial property towards various types of bacteria strains such as *Bacillus subtilis* and *Escherichia coli* (E.coli) [45]. Recent study by Wang et al. also reported that ZnO-GO composites were superb antibacterial materials to effectively inhibit various kinds of bacterial growth and propagation [46]. Owing to the distinct advantages of ZnO NPs in eliminating a broad spectrum of pathogens or microorganisms, it was used in the evaluation of the membranes antibacterial properties. The FESEM images in Fig. 10 exhibited the bacterial growth on 3 different types of membranes, i.e. P0, Z2 and ZG3. Obviously, the bacterial colonies were reduced significantly after 1 night of incubation in PSF-ZnO and PSF-ZnO-GO membranes compared to the blank PSF membrane with a large colony of bacteria. According to Sirelkhatim et al., the antibacterial mechanisms could be attributed to the direct contact of ZnO NPs with bacteria cell walls, resulting in bacterial cell integrity disruption, and also Reactive Oxygen Species (ROS) generation which would release hydrogen peroxide, hydroxide and superoxide anion [47]. Besides, the study by Kochkodan et al. (2006) stated that there would be less adhesion of E.coli on hydrophilic membrane surface which was in good agreement with the findings obtained in this study. The enhanced antimicrobial control could also be explained based on membrane surface roughness due to smoother surface with less occurrence of hills and valleys would easily remove bacterium cells [48]. The combination of ZnO and GO NPs was a great effort in maximizing the antibacterial ability, owing to the benefits of GO to serve as a better platform to facilitate for ZnO dispersion [46]. It could be assumed that the PSF-ZnO-GO membrane yield the best antibacterial properties due to its ability to eradicate most of the E.coli cells due to the synergistic effects of ZnO-GO which enhanced the electron transfer to contribute on more ROS formation in eliminating the bacterial cells. Hence, the practicability of ZnO and ZnO-GO incorporated membranes in bacterial growth inhibition was successfully proven with great performance. The enriched antimicrobial properties of these membranes could be further utilized in various kinds of separation and purification applications involving bio-fouling issues.

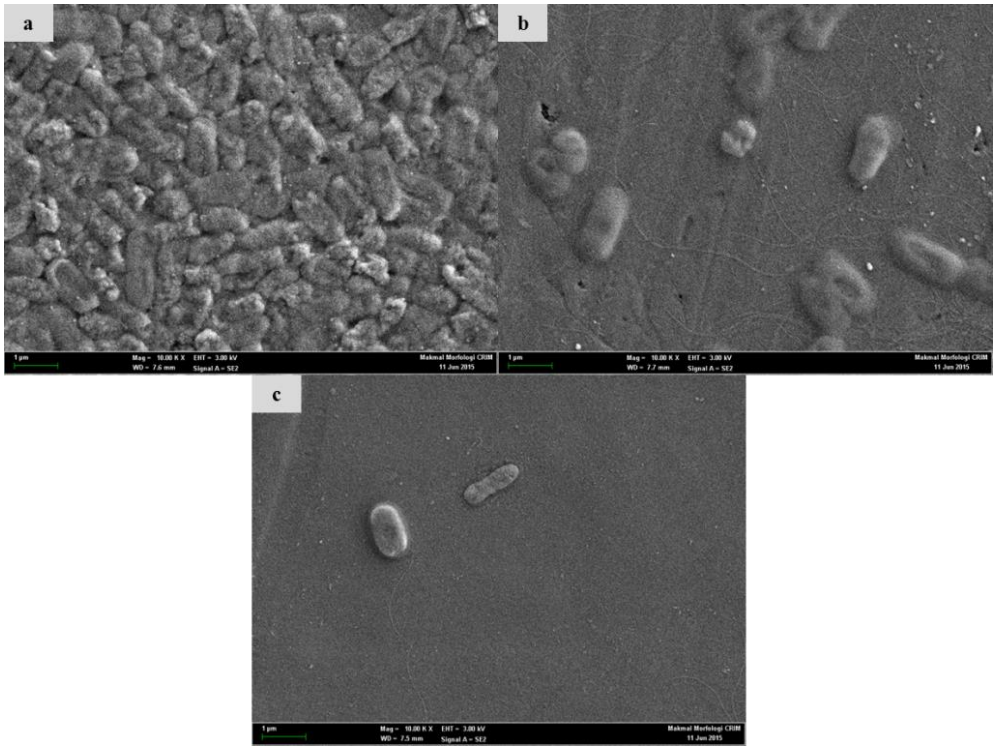

Fig. 10. FESEM images for membranes with E-coli antibacterial test: a) Pure PSF [P0] b) PSF-ZnO [Z2] c) PSF-ZnO/GO [ZG3].

4. Significance of study

Generally, the fabrication of membranes with the incorporation of various concentrations of ZnO and ZnO-GO NPs were performed successfully. The membrane performance and characterization studies demonstrated that the significance of the incorporation of hydrophilic nanoparticles towards the enhancement of membranes properties. From this study, the best performance of membrane was illustrated in Z2 membrane with ZnO NPs and ZG3 membrane with ZnO-GO NPs. The novelty of this study was that the functionalization of ZnO NPs with GO nanosheets contributed to the significant membrane performance improvement due to its homogeneous dispersion and increased hydrophilic nature of the membranes. The ZnO dispersed onto GO nanosheets could be reduced by 5 times while exhibiting excellent performance. The ZnO-GO composite membranes are the most hydrophilic membranes with lowest contact angle value in comparison with other GO-composite with TiO_2, SiO_2 and Ag. This is an encouraging phenomenon as the findings from this study provide an essential alternative towards the production of better membrane properties with the hydrophilic ZnO NPs and further distribution enhancement in membrane matrix with GO nanofillers. In addition, the excellent antifouling and antimicrobial properties of these ZnO-nanohybrid membranes are essential in the prevention of fouling biofilm formation and thus enhancing the process efficiency in various separation applications especially overcoming the severe biofouling issues in desalination technology.

5. Conclusion

The Polysulfone-nanohybrid membranes were successfully fabricated with ZnO nanoparticles and functionalized ZnO on the GO nanosheets surface. Both kinds of nanoparticles were hydrophilic in nature due to the polar characteristics of ZnO and abundance of hydroxyl, carbonyl and epoxy groups from GO. The unique characteristics of ZnO and ZnO-GO NPs were verified with several analyses, i.e. XRD, TEM and FESEM. The enhancement of membranes was investigated by varying the concentrations of the NPs. The optimum membrane performance was exhibited by PSF-ZnO 2 wt% (Z2) membrane and PSF-ZnO-GO 0.6 wt% (ZG3) membrane. Both membranes illustrated significant enhancement in terms of hydrophilicity, permeability, porosity, pore size, rejection tendency and fouling propensity. The membrane hydrophilicity decreased from 65° (P0) to 39° (Z2 & ZG3) while membrane permeability increased from 0.89 (P0) to 2.83 (Z2) and 5.11 (ZG3) $L.m^{-2}.h^{-1}.bar^{-1}$ respectively. The membrane porosity also improved from 75% to 90% for ZG3 membrane. Besides, the humic acid rejection for both Z2 and ZG3 membrane were approaching 96% and 99% with greatly enhanced antifouling properties. Antibacterial testing was performed with E.coli to examine the practicability of these nanohybrid membranes in overcoming bio-fouling problems. The final goal of this study is to investigate the improvement of membrane properties with the pure ZnO and GO-functionalized ZnO NPs. The ZnO NPs were minimal in size which might cause less agglomeration. However, the GO-functionalized ZnO NPs were highly favourable since GO had a better interface for ZnO dispersion. Hence, it could be concluded that the incorporation of both ZnO and ZnO-GO NPs into PSF membranes was an advanced approach in creating better membranes with significant hydrophilicity and fouling control enhancement which was suitable in various separation and purification applications.

Acknowledgment

This study was financially supported by the NPRP grant # [5-1425-2-607] from the Qatar National Research Fund (a member of Qatar Foundation). The statements made herein are solely the responsibility of the authors. In addition, the authors wish to acknowledge the Ministry of Education Malaysia for sponsoring the postgraduate study of Y.T. Chung through the MyBrain15 program. The CRIM (Centre for Research and Instrumentation Management, UKM) is also acknowledged for XRD, FESEM and TEM analyses.

References

[1] B. Van der Bruggen, M. Mänttäri, M. Nyström, Drawbacks of applying nanofiltration and how to avoid them: A review, Sep. Purif. Technol. 63 (2008) 251–263. doi:10.1016/j.seppur.2008.05.010.

[2] A.W. Mohammad, N. Hilal, M. Nizam Abu Seman, A study on producing composite nanofiltration membranes with optimized properties, Desalination. 158 (2003) 73–78. doi:10.1016/S0011-9164(03)00435-1.

[3] A.A. Abuhabib, A.W. Mohammad, N. Hilal, R.A. Rahman, A.H. Shafie, Nanofiltration membrane modification by UV grafting for salt rejection and fouling resistance improvement for brackish water desalination, Desalination. 295 (2012) 16–25. doi:10.1016/j.desal.2012.03.020.

[4] E. Kim, Q. Yu, B. Deng, Plasma surface modification of nanofiltration (NF) thin-film composite (TFC) membranes to improve anti organic fouling, Appl. Surf. Sci. 257 (2011) 9863–9871. doi:10.1016/j.apsusc.2011.06.059.

[5] A. Linggawati, A.W. Mohammad, C.P. Leo, Effects of APTEOS content and electron beam irradiation on physical and separation properties of hybrid nylon-66 membranes, Mater. Chem. Phys. 133 (2012) 110–117. doi:10.1016/j.matchemphys.2011.12.071.

[6] L.Y. Ng, A.W. Mohammad, C.Y. Ng, C.P. Leo, R. Rohani, Development of nanofiltration membrane with high salt selectivity and performance stability using polyelectrolyte multilayers, Desalination. 351 (2014) 19–26. doi:10.1016/j.desal.2014.07.020.

[7] L.Y. Ng, A.W. Mohammad, C.P. Leo, N. Hilal, Polymeric membranes incorporated with metal/metal oxide nanoparticles: A comprehensive review, Desalination. 308 (2013) 15–33. doi:http://dx.doi.org/10.1016/j.desal.2010.11.033.

[8] S. Horikoshi, N. Serpone, Introduction to Nanoparticles, in: Microwaves Nanoparticles Synth., First Edit, Wiley-VCH Verlag GmbH & Co.KGaA, 2013: pp. 1–24.

[9] S. Balta, A. Sotto, P. Luis, L. Benea, B. Van der Bruggen, J. Kim, A new outlook on membrane enhancement with nanoparticles: The alternative of ZnO, J. Memb. Sci. 389 (2012) 155–161. doi:http://dx.doi.org/10.1016/j.memsci.2011.10.025.

[10] M. Vaseem, A. Umar, Y. Hahn, ZnO Nanoparticles : Growth , Properties , and Applications, in: Met. Oxide Nanostructures Their Appl., American Scientific, 2010: pp. 1–36.

[11] L. Shen, X. Bian, X. Lu, L. Shi, Z. Liu, L. Chen, et al., Preparation and characterization of ZnO/polyethersulfone (PES) hybrid membranes, Desalination. 293 (2012) 21–29. doi:10.1016/j.desal.2012.02.019.

[12] S. Liang, K. Xiao, Y. Mo, X. Huang, A novel ZnO nanoparticle blended polyvinylidene fluoride membrane for anti-irreversible fouling, J. Memb. Sci. 394-395 (2012) 184–192. doi:10.1016/j.memsci.2011.12.040.

[13] S. Zhao, W. Yan, M. Shi, Z. Wang, J. Wang, S. Wang, Improving permeability and antifouling performance of polyethersulfone ultrafiltration membrane by incorporation of ZnO-DMF dispersion containing nano-ZnO and polyvinylpyrrolidone, J. Memb. Sci. 478 (2015) 105–116. doi:10.1016/j.memsci.2014.12.050.

[14] X. Zhang, Y. Wang, Y. Liu, J. Xu, Y. Han, X. Xu, Preparation, performances of PVDF/ZnO hybrid membranes and their applications in the removal of copper ions,

Appl. Surf. Sci. 316 (2014) 333–340. doi:10.1016/j.apsusc.2014.08.004.

[15] C.P. Leo, C.W.P. Lee, A.L. Ahmad, A.W. Mohammad, Polysulfone membranes blended with ZnO nanoparticles for reducing fouling by oleic acid, Sep. Purif. Technol. 89 (2012) 51–56. doi:http://dx.doi.org/10.1016/j.seppur.2012.01.002.

[16] Y. Jafarzadeh, R. Yegani, M. Sedaghat, Preparation, characterization and fouling analysis of ZnO/polyethylene hybrid membranes for collagen separation, Chem. Eng. Res. Des. (2014) 1–11. doi:10.1016/j.cherd.2014.08.017.

[17] J. Hong, Y. He, Polyvinylidene fluoride ultrafiltration membrane blended with nano-ZnO particle for photo-catalysis self-cleaning, Desalination. 332 (2014) 67–75. doi:10.1016/j.desal.2013.10.026.

[18] Q. Bao, D. Zhang, P. Qi, Synthesis and characterization of silver nanoparticle and graphene oxide nanosheet composites as a bactericidal agent for water disinfection, J. Colloid Interface Sci. 360 (2011) 463–470. doi:10.1016/j.jcis.2011.05.009.

[19] J.J. Song, Y. Huang, S.-W. Nam, M. Yu, J. Heo, N. Her, et al., Ultrathin graphene oxide membranes for the removal of humic acid, Sep. Purif. Technol. 144 (2015) 162–167. doi:10.1016/j.seppur.2015.02.032.

[20] Z. Wang, H. Yu, J. Xia, F. Zhang, F. Li, Y. Xia, et al., Novel GO-blended PVDF ultrafiltration membranes, Desalination. 299 (2012) 50–54. doi:10.1016/j.desal.2012.05.015.

[21] X.-F. Sun, J. Qin, P.-F. Xia, B.-B. Guo, C.-M. Yang, C. Song, et al., Graphene oxide–silver nanoparticle membrane for biofouling control and water purification, Chem. Eng. J. 281 (2015) 53–59. doi:10.1016/j.cej.2015.06.059.

[22] V. Vatanpour, A. Shockravi, H. Zarrabi, Z. Nikjavan, A. Javadi, Fabrication and characterization of anti-fouling and anti-bacterial Ag-loaded graphene oxide/polyethersulfone mixed matrix membrane, J. Ind. Eng. Chem. (2015) 1–11. doi:10.1016/j.jiec.2015.06.004.

[23] H. Wu, B. Tang, P. Wu, Development of novel SiO2-GO nanohybrid/polysulfone membrane with enhanced performance, J. Memb. Sci. 451 (2014) 94–102. doi:10.1016/j.memsci.2013.09.018.

[24] M. Safarpour, V. Vatanpour, A. Khataee, Preparation and characterization of graphene oxide/TiO2 blended PES nanofiltration membrane with improved antifouling and separation performance, Desalination. (2015). doi:10.1016/j.desal.2015.07.003.

[25] M. Safarpour, A. Khataee, V. Vatanpour, Thin film nanocomposite reverse osmosis membrane modified by reduced graphene oxide/TiO2 with improved desalination performance, J. Memb. Sci. 489 (2015) 43–54. doi:10.1016/j.memsci.2015.04.010.

[26] Y.-L. Chen, C.-E. Zhang, C. Deng, P. Fei, M. Zhong, B.-T. Su, Preparation of ZnO/GO composite material with highly photocatalytic performance via an improved two-step method, Chinese Chem. Lett. 24 (2013) 518–520. doi:10.1016/j.cclet.2013.03.034.

[27] R. Rezaee, S. Nasseri, A.H. Mahvi, R. Nabizadeh, S.A. Mousavi, A. Rashidi, et al., Fabrication and characterization of a polysulfone-graphene oxide nanocomposite membrane for arsenate rejection from water, J. Environ. Heal. Sci. Eng. 13 (2015) 61. doi:10.1186/s40201-015-0217-8.

[28] M. Safarpour, V. Vatanpour, A. Khataee, M. Esmaeili, Development of a novel high flux and fouling-resistant thin film composite nanofiltration membrane by embedding

reduced graphene oxide/TiO2, Sep. Purif. Technol. 154 (2015) 96–107. doi:http://dx.doi.org/10.1016/j.seppur.2015.09.039.

[29] E. Mahmoudi, L.Y. Ng, M.M. Ba-Abbad, A.W. Mohammad, Novel Nanohybrid Polysulfone Membrane Embedded with Silver Nanoparticles on Graphene Oxide Nanoplates, Chem. Eng. J. 277 (2015) 1–10. doi:10.1016/j.cej.2015.04.107.

[30] Y.T. Chung, M.M. Ba-Abbad, A.W. Mohammad, N.H.H. Hairom, A. Benamor, Synthesis of minimal-size ZnO nanoparticles through sol-gel method: Taguchi design optimisation, Mater. Des. 87 (2015) 780–787. doi:10.1016/j.matdes.2015.07.040.

[31] COMPRES Technology Center, Introduction of JCPDS Card, COMPRES. (2015). http://comptech.compres.us/tools/jcpds/.

[32] A.R. Marlinda, N.M. Huang, M.R. Muhamad, M.N. An'Amt, B.Y.S. Chang, N. Yusoff, et al., Highly efficient preparation of ZnO nanorods decorated reduced graphene oxide nanocomposites, Mater. Lett. 80 (2012) 9–12. doi:10.1016/j.matlet.2012.04.061.

[33] L. Stobinski, B. Lesiak, A. Malolepszy, M. Mazurkiewicz, B. Mierzwa, J. Zemek, et al., Graphene oxide and reduced graphene oxide studied by the XRD, TEM and electron spectroscopy methods, J. Electron Spectros. Relat. Phenomena. 195 (2014) 145–154. doi:10.1016/j.elspec.2014.07.003.

[34] R. Nackaerts, Are membranes implemented with nanoparticles able to provide a breakthrough in water purification ?, Universiteit Gent, 2014.

[35] V. Vatanpour, S.S. Madaeni, R. Moradian, S. Zinadini, B. Astinchap, Fabrication and characterization of novel antifouling nanofiltration membrane prepared from oxidized multiwalled carbon nanotube/polyethersulfone nanocomposite, J. Memb. Sci. 375 (2011) 284–294. doi:10.1016/j.memsci.2011.03.055.

[36] H. Rajabi, N. Ghaemi, S.S. Madaeni, P. Daraei, B. Astinchap, S. Zinadini, et al., Nano-ZnO embedded mixed matrix polyethersulfone (PES) membrane: Influence of nanofiller shape on characterization and fouling resistance, Appl. Surf. Sci. 349 (2015) 66–77. doi:10.1016/j.apsusc.2015.04.214.

[37] M. Alhoshan, J. Alam, L.A. Dass, N. Al-Homaidi, Fabrication of polysulfone/ZnO membrane: Influence of ZnO nanoparticles on membrane characteristics, Adv. Polym. Technol. 32 (2013) 1–7. doi:10.1002/adv.21369.

[38] Y.T. Chung, M.M. Ba-Abbad, A.W. Mohammad, A. Benamor, Functionalization of zinc oxide (ZnO) nanoparticles and its effects on polysulfone-ZnO membranes, Desalin. Water Treat. 57 (2015) 1–11. doi:10.1080/19443994.2015.1067168.

[39] M. Safarpour, A. Khataee, V. Vatanpour, Preparation of a novel polyvinylidene fluoride (PVDF) ultrafiltration membrane modified with reduced graphene oxide/titanium dioxide (TiO2) nanocomposite with enhanced hydrophilicity and antifouling properties, Ind. Eng. Chem. Res. 53 (2014) 13370–13382. doi:10.1021/ie502407g.

[40] A.L. Ahmad, A.A. Abdulkarim, S. Ismail, B.S. Ooi, Preparation and characterisation of PES-ZnO mixed matrix membranes for humic acid removal, Desalin. Water Treat. 54 (2014) 1–12. doi:10.1080/19443994.2014.910137.

[41] G. Williams, B. Seger, P. V Kamat, TiO2-Graphene Nanocomposites. UV-Assisted Photocatalytic Reduction of Graphene Oxide, ACS Nano. 2 (2008) 1487–1491.

[42] Y.H. Teow, B.S. Ooi, A.L. Ahmad, J.K. Lim, Mixed-Matrix Membrane for Humic

Acid Removal: Influence of Different Types of TiO2 on Membrane Morphology and Performance, Int. J. Chem. Eng. Appl. 3 (2012) 374–379. doi:10.7763/IJCEA.2012.V3.222.

[43] Y.T. Chung, L.Y. Ng, A.W. Mohammad, Sulfonated-polysulfone membrane surface modification by employing methacrylic acid through UV-grafting: Optimization through response surface methodology approach, J. Ind. Eng. Chem. 20 (2014) 1549–1557. doi:10.1016/j.jiec.2013.07.046.

[44] M.J. Hajipour, K.M. Fromm, A.A. Ashkarran, D.J. de Aberasturi, I.R. de Larramendi, T. Rojo, et al., Antibacterial properties of nanoparticles., Trends Biotechnol. 30 (2012) 499–511. doi:10.1016/j.tibtech.2012.06.004.

[45] H. Meruvu, V. Meena, S.C. Chippada, S.R. Bammidi, Synthesis and Characterization of Zinc Oxide Nanoparticles and Its Antimicrobial Activity against Bacillus Subtilis and Escherichia Coli, RASAYAN J.Chem. 4 (2011) 217–222.

[46] Y.W. Wang, A. Cao, Y. Jiang, X. Zhang, J.H. Liu, Y. Liu, et al., Superior antibacterial activity of zinc oxide/graphene oxide composites originating from high zinc concentration localized around bacteria, ACS Appl. Mater. Interfaces. 6 (2014) 2791–2798. doi:10.1021/am4053317.

[47] A. Sirelkhatim, S. Mahmud, A. Seeni, N.H.M. Kaus, L.C. Ann, S.K.M. Bakhori, et al., Review on Zinc Oxide Nanoparticles: Antibacterial Activity and Toxicity Mechanism, Nano-Micro Lett. 7 (2015) 219–242. doi:10.1007/s40820-015-0040-x.

[48] V.M. Kochkodan, N. Hilal, V. V. Goncharuk, L. Al-Khatib, T.I. Levadna, Effect of the surface modification of polymer membranes on their microbiological fouling, Colloid J. 68 (2006) 267–273. doi:10.1134/S1061933X06030021.

[49] H. Rabiee, V. Vatanpour, M.H.D.A. Farahani, H. Zarrabi, Improvement in flux and antifouling properties of PVC ultrafiltration membranes by incorporation of zinc oxide (ZnO) nanoparticles, Sep. Purif. Technol. 156 (2015) 299–310. doi:10.1016/j.seppur.2015.10.015.

[50] M. Kumar, Z. Gholamvand, A. Morrissey, K. Nolan, M. Ulbricht, J. Lawler, Preparation and characterization of low fouling novel hybrid ultrafiltration membranes based on the blends of GO−TiO2 nanocomposite and polysulfone for humic acid removal, J. Memb. Sci. 506 (2016) 38–49. doi:10.1016/j.memsci.2016.02.005.